A constitutive model for cemented clays capturing cementation degradation

Lam Nguyen[1], Behzad Fatahi[2*] and Hadi Khabbaz[3]

[1] PhD Candidate (MEng, BEng(hons)), School of Civil and Environmental Engineering, University of Technology Sydney (UTS), Sydney, Australia

[2] Senior Lecturer of Geotechnical Engineering (PhD, MEng, BEng, CPEng, NPER), School of Civil and Environmental Engineering, University of Technology Sydney (UTS), Sydney, Australia

[3] Associate Professor of Geotechnical Engineering (PhD, MEng, BEng), School of Civil and Environmental Engineering, University of Technology Sydney (UTS), Sydney, Australia

**Corresponding Author, School of Civil and Environmental Engineering*

Faculty of Engineering and Information Technology

University of Technology, Sydney (UTS)

City Campus PO Box 123 Broadway NSW 2007

T (+61) (2) 9514 7883 F (+61) (2) 9514 2633 M 0413573481

Email: behzad.fatahi@uts.edu.au

NOTATIONS

A	Derivative of p'^{*} with respect to p'
α	non dimensional anisotropic parameter
β	Cementation degradation parameter
CSL	Critical state line
C	Shear strength contributed by cementation when $p' = 0$
d_v	Total volumetric strain increment
$d_v{}^e$	Elastic volumetric strain increment
$d_v{}^p$	Plastic volumetric strain increment
d_ε	Total plastic deviatoric strain increment
$d_\varepsilon{}^e$	Elastic deviatoric strain increment
$d_\varepsilon{}^p$	Plastic deviatoric strain increments
dW_{in}	Internal plastic energy per unit volume
e	Void ratio of the soil
ε_1	Axial strain
ε_3	Radial strain
f	Yield function
g	Plastic potential function
κ	Swelling or recompression index
λ	Compression index
M	Slope of failure envelope of reconstituted soil
η	Stress ratio
η^*	Modified stress ratio
ν	Poisson's ratio

p'	Mean effective stress
p'^*	Modified mean effective stress
p'^*_0	Modified mean effective stress on the yield surface when q = 0
$p'^*_{0,i}$	Initial size of the yield surface
p'_0	Hardening parameter – mean effective stress on the yield surface when q = 0
$p'_{y,i}$	Initial mean effective yield stress
p'_Ω	p′(tension) when q = 0, describing the effect of cementation
ψ^*	Proposed flow rule
q	Deviatoric stress
q_u	Unconfined compressive strength
σ'_1	Axial effective stress
σ'_3	Radial effect stress

ABSTRACT

Laboratory experiments show that the effect of cementation on clays gradually diminishes as the confining pressure increases (particularly at high confining pressures) due to the degradation of cementation bonds. The main aim of this paper is to propose a constitutive model for cemented clays, referred to as the Cemented Cam Clay model (CCC), to simulate the cementation degradation during loading. The failure envelope of the proposed model is formulated to describe the behaviour of the cemented clay at a low pressure range similar to over-consolidated soils, while it merges with the Critical State Line of reconstituted sample gradually as the confining pressure continues to increase. In order to examine the stress-strain behaviour of cemented clays, an energy dissipation equation is developed inspired by the Modified Cam Clay model. The characteristics of the proposed model, including a non-associated plastic potential function and elasto-plastic stress-strain relationship, are presented in light of the Critical State concept. Validity of the proposed constitutive model derived from the modified energy equation is evaluated against triaxial test results for cemented clays available in literature.

KEY WORDS: A. yield condition, B. elastic-plastic material, B. constitutive behaviour , C. analytic functions

1. INTRODUCTION

With the growth of cities and industries, suitable sites, which can be used without some ground modification, are becoming increasingly scarce. Moreover, the cost of replacing soft soils with high quality material has dramatically increased. The design engineers have various options in dealing with problematic soils such as bypassing the poor soil, replacing it with superior soil, redesigning the structure for the poor condition or improving the soil properties by mixing soil with material such as cement, lime, gypsum and fly ash among other ground modification techniques. The latter option can be used for surface improvement, such as road and rail subgrade improvement, or in deep soil mixing or jet grouting technologies, which are soil improvement approaches, mixing in situ soil with strengthening agents.

A number of laboratory experiments on the effect of cementation have resulted in several constitutive models for cemented clays (Horpibulsuk et al., 2010; Kasama et al., 2000; Liu and Carter, 2002; Yasufuku et al., 1997). Kasama et al. (2000) proposed a constitutive model for cemented clays extending the critical state concept by introducing the cementation effect into the energy dissipation equation. They also modified the Critical State concept to include the increase in the strength of the clay, which results in extending the stress domain. Horpibulsuk et al. (2010) simulated the behaviour of cemented clays via the framework of the Structured Cam Clay (SCC) model developed by Liu and Carter (2002). Their constitutive model is an extension of SCC model for cemented clays by modifying the mean effective stress, while the effect of cementation is considered to reinforce the mean effective stress (Horpibulsuk et al., 2010). The failure envelope of the extended SCC model has been assumed to be parallel to that of untreated clay and shifted by a certain intercept, which characterises the effect of cementation similar to the model proposed by Kasama et al. (2000). Although these models provide a conceptual framework for the development of an appropriate constitutive model capturing the behaviour of cemented clays, the effect of cementation degradation due to the increase in the confining pressure has not been captured in these models. As suggested by Moses et al. (2003); Panda and Rao (1998) and Lo and Wardani (1999), when the confining pressure increases, the beneficial effects of cementation may diminish as a result of cementation degradation. Therefore, the failure envelope of the cemented clay gradually merges with that of reconstituted clay-cement mixture.

The aim of this paper is to propose an enhanced model to simulate the behaviour of cemented clays under various confining pressures. The degradation of cementation bonds due to increasing confining pressure is presented by a non-linear failure envelope of cemented clay, merging to that of reconstituted soil in high confining pressure. The development of this model is mainly based on the Modified Cam Clay (MCC) model, and when there is no effect of cementation, the model returns to its original form. The paper introduces a new plastic potential function developed through modifying the energy dissipation equation. In addition, a modified stress-strain relationship for cemented clays is presented.

2. FACTORS AFFECTING THE STRENGTH OF CEMENTED CLAY

As proposed by Diamond and Kinter (1965) and confirmed by several other researchers such as Kamruzzaman et al. (2006); Porbaha (1998) and Chew et al. (2004), the three major categories of reactions, expected in the process of mixing a stabiliser with clay, are: (i) dehydration process, (ii) ion exchange or flocculation and (iii) pozzolanic reaction. Lorenzo and Bergado (2006) explained that the hydration process occurs rapidly when cement is mixed with pore water of the soil to form primary cementitious products such as hydparameterd calcium aluminates and hydparameterd lime. These cementing products result in the dissociation of calcium ions which then react with soil silica and alumina to form pozzolanic products. This secondary cementing product, stabilising the soil and increasing the strength of improved soil with time, is also reported by Porbaha et al. (2000).

Laboratory experiments have been conducted broadly by various researchers to report different factors affecting the strength of cemented clays (Lorenzo and Bergado, 2006; Porbaha et al., 2000; Tan et al., 2002; Uddin et al., 1997). According to Tan et al. (2002), there is a linear relationship between the amount of stabilising agents, such as lime and cement, and the strength of the improved clay. The unconfined compressive strength (q_u) generally increases with increasing the cement content and the curing time for a fixed amount of water content (Lorenzo and Bergado, 2006), especially for cement contents greater than 5% as observed by Sariosseiri and Muhunthan (2009) and Uddin et al. (1997). The effect of increasing cement content on the strength of improved soils is mainly due to the pozzolanic reactions (Lorenzo and Bergado, 2006). However, expectedly, the water content has an inverse effect on the compressive strength of the soil at any particular cement content (Porbaha et al., 2000). Similar to concrete, the strength of the cemented clay is commonly accepted to develop with curing time (e.g. Porbaha et al. (2000); Uddin et al. (1997)). Thus,

the effects of increasing cement content and aging at particular water content play significant roles in the strength development of cemented clays.

The confining pressure is also an important parameter, influencing the behaviour of cemented clay (Uddin et al., 1997). As reported by Lorenzo and Bergado (2006), the experimental results from triaxial tests show that increasing the confining pressure leads to an increase in the deviatoric stress at failure; this is even more significant at higher cement contents. Unlike the ductile behaviour of untreated clays, the cemented clays generally exhibit more brittle behaviour as the stress increases to the peak strength state and then drop to the residual strength at the post-peak state (Lorenzo and Bergado, 2006; Porbaha et al., 2000; Yin, 2001). This indicates that the behaviour of cemented clay is similar to over-consolidated soil and the cemented clay is more structured due to chemically induced cementation (Panda and Rao, 1998; Yin, 2001). Lade and Overton (1989) proposed a non-linear failure envelope for cemented clays, which is positioned significantly higher than that of untreated soil in $p' - q$ graph. The cementation increases the friction angle and the cohesion of the soil and the cemented clays behave like over-consolidated soil at low confining pressures. However, the high stiffness of cemented clays restricts their compressibility during consolidation compared to untreated clays. Thus, as the confining pressure continues to increase, the effect of cementation on the strength of the cemented clay keeps reducing due to cracking and degradation of cementation bonds (Lade and Overton, 1989). Uddin et al. (1997) also observed that the apparent over-consolidation ratio of the soil is reduced as the beneficial effect of cementation is diminished under sufficiently high confining pressures. Due to increasing microcracks in cementation as the confining stress increases, the undrained strength is reduced significantly as the soil structure is progressively changed. As a result, the failure envelope of cemented clays gradually approaches to the remoulded clay-cement mixture as observed by Moses et al. (2003); Panda and Rao (1998) and Lo and Wardani (1999). Figure 1 displays triaxial test laboratory data on Indian marine clay mixed with 3% hydparameterd lime. Results clearly indicate that a collection of failure points of cemented clay forms a non-linear failure envelope, which is not parallel to the Modified Cam Clay failure envelope ($q = Mp'$). For the sake of simplicity, Structured Cam Clay (SCC) model (Horpibulsuk et al., 2010; Liu and Carter, 2002) assumes a linear failure line parallel to that of reconstituted soil. In other words, SCC model ignores the reduction in the strength of the cemented clay due to degradation of cementation bonds as a result of confining pressure increase.

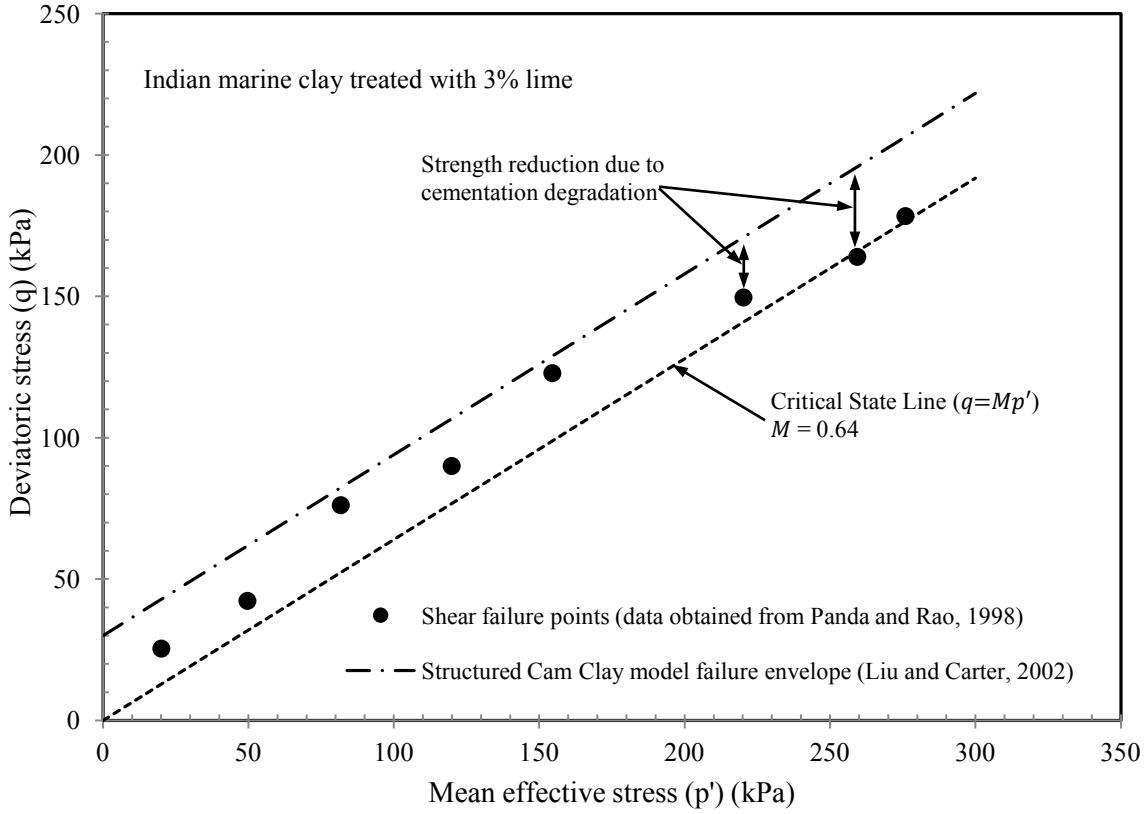

Figure 1. Failure envelope for artificially cemented Indian marine clay

3. DEVELOPMENT OF CEMENTED CAM CLAY MODEL

3.1. Modified mean effective stress

In this paper, the definition of stress and strain quantities similar to Modified Cam Clay model for conventional triaxial test is adopted (Roscoe and Burland, 1968) as explained below:

- The mean effective stress (p'), the deviatoric stress (q), and the stress ratio (η) are given by:

$$p' = \frac{\sigma'_1 + 2\sigma'_3}{3} \tag{1}$$

$$q = \sigma'_1 - \sigma'_3 \tag{2}$$

$$\eta = \frac{q}{p'} \tag{3}$$

- The volumetric strain increment (d_v) and the deviatoric strain increment (d_ε) are defined as follows:

$$d_v = d\varepsilon_1 + 2d\varepsilon_3 \tag{4}$$

$$d_\varepsilon = \frac{2(d\varepsilon_1 - d\varepsilon_3)}{3} \tag{5}$$

where, σ'_1 and $d\varepsilon_1$ are axial effective stress and the axial strain increment, respectively, and, σ'_3 and $d\varepsilon_3$ are radial effective stress and the radial strain increment, respectively.

Based on the framework of the Critical State Soil Mechanics and the basis of MCC model, the proposed model has modified the mean effective stress so that the effect of cementation is clearly obtained and analysed while incorporating destructurisation as a function of mean effective stress. In other words, the mean effective stress is strengthened by cementation, similar to cohesionless soil (Horpibulsuk et al., 2010; Kasama et al., 2000), while incorporating cementation degradation with increasing mean effective stress. The modified mean effective stress (p'^*) is proposed to introduce the effect of cementation and its degradation as follows:

$$p'^* = p' + p'_\Omega \tag{6}$$

$$p'_{\Omega} = \frac{C(1+\frac{p'}{C+\beta})exp^{\left(\frac{-p'}{C+\beta}\right)}}{M} \quad (7)$$

where, p'_{Ω} is a function of p' describing the effect of cementation, M is the slope of failure envelope of reconstituted clay-cement mixture and C represents the contribution of the cementation to the shear strength when the mean effective stress is zero. The model fitting parameter (β) influences the degradation rate of cementation due to the mean effective stress. When the modified mean effective stress is proposed, the stress ratio (η^*) needs to be modified as follows:

$$\eta^* = \frac{q}{p'^*} \quad (8)$$

3.2. Proposed failure envelope

Considering the modified mean effective stress proposed in Equation (6), the failure envelope of the Cemented Cam Clay model is also modified to capture the degradation effect of cementation [$q = M(p' + p'_{\Omega})$]. Thus, the failure envelope is taking the form of:

$$q = Mp' + C(1 + \frac{p'}{C+\beta})exp^{\left(\frac{-p'}{C+\beta}\right)} \quad (9)$$

Moses et al. (2003) has indicated that the behaviour of cemented clay depends on the strength of cementation, and the bond strength depends upon the stress level within the soil, and other factors such as strain parameter and type of loading. In this study, p'_{Ω} is proposed in a way that as the mean effective stress (p') increases to a sufficiently high pressure, p'_{Ω} approaches zero since the effect of cementation is diminished. As a result, the modified mean effective stress can replace the mean effective stress to simulate the behaviour of cemented clays. In Equation (7), when C = 0 (no binding agent), the effect of cementation prevails $\left(p'_{\Omega} = 0\right)$ and Equation (9) converts to MCC model ($q = Mp'$). Figure 2 illustrates the proposed failure envelope for cemented clay compared to that of reconstituted clay-cement mixture and Structured Cam Clay model proposed by Horpibulsuk et al. (2010). The amount of cementation is significantly reduced to residual strength and diminishes as the failure envelope approaches the Critical State Line ($q = Mp'$). It can be noted that the Structured Cam Clay model (Horpibulsuk et al., 2010) considers a constant increase in the shear strength

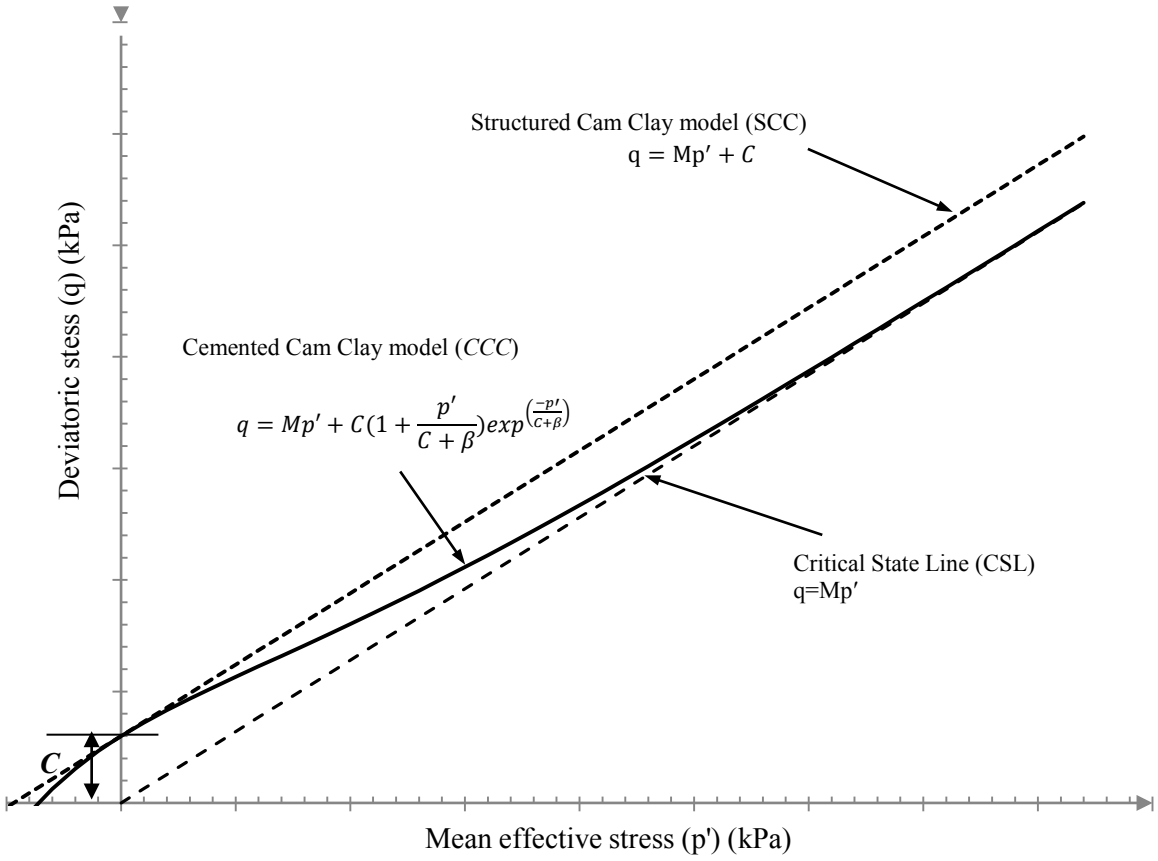

Figure 2. Proposed failure envelope compared with Structured Cam Clay model and The Critical State line

(or deviatoric stress at failure) due to cementation ($q = Mp' + C$) and cementation degradation under high mean effective stresses has been ignored.

Figure 3 displays a predicted failure envelope (Equation 9) for a set of triaxial tests from Indian marine clay performed by Panda and Rao (1998). A dramatic increase in the unconfined compressive strength (q_u) of the clay improved with 3% hydrated lime is observed from 12 kPa to 58 kPa. As presented in Figure 3, with an increase in the confining pressure, the contribution of cementation to the shear strength is gradually reduced, and the failure envelope finally merges with the failure envelope of the reconstituted clay-cement mixture with C = 0 and $M = 0.64$. The failure envelope proposed in this study captures the merging effect of cemented clay with the reconstituted clay-cement mixture, as a result of cementation degradation, reasonably well. The effects of increasing model parameters, *C* and β on the predicted failure envelope of the proposed model are shown in Figures 4 and 5, respectively.

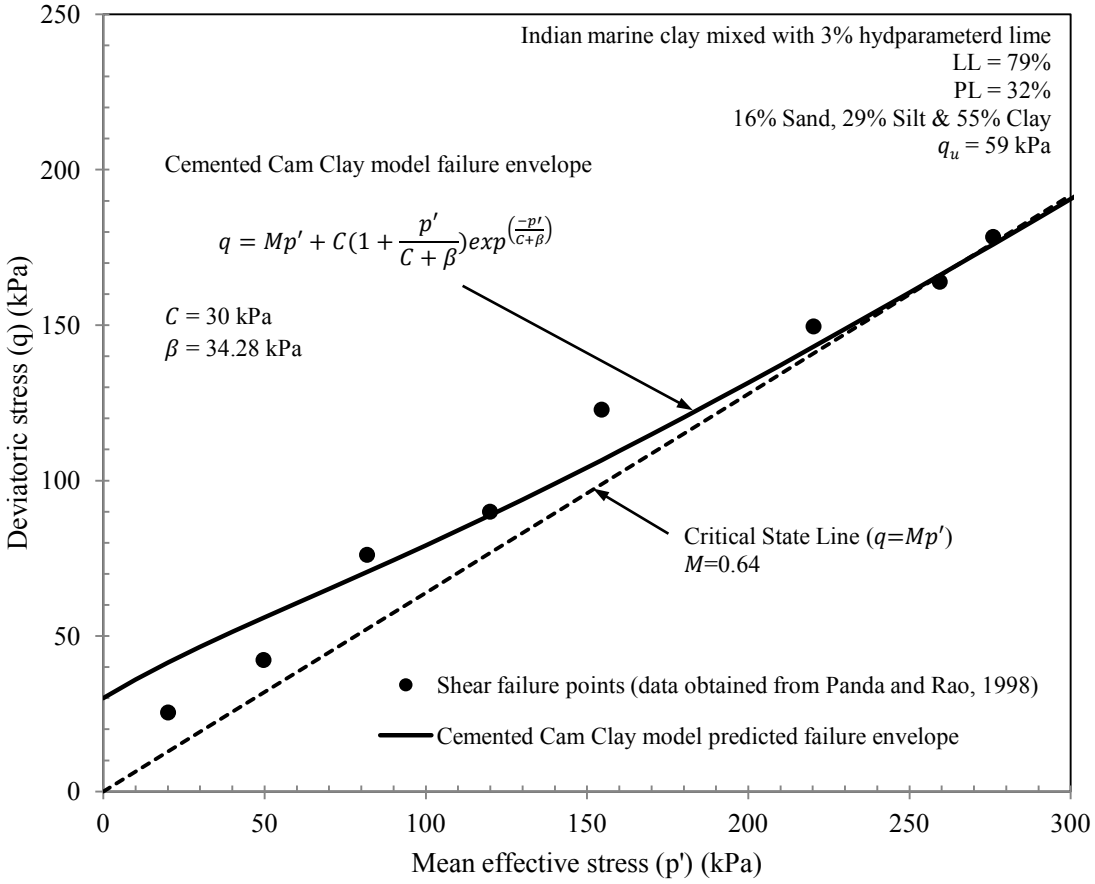

Figure 3. Predicted failure envelope for 3% cemented Indian marine clay

Referring to Figure 4, by keeping the parameter β constant at 34.28 kPa, when there is no cementation effect (C = 0), the failure envelope of proposed model converts to Critical State Line ($q = Mp'$). As the effect of cementation increases (increasing C), higher values of q are obtained at a particular mean effective stress on the proposed failure envelope. Moreover, the tensile strength also increases with the increase in cementation. However, the value of q gradually approaches the Critical State Line at higher confining pressures due to cementation degradation.

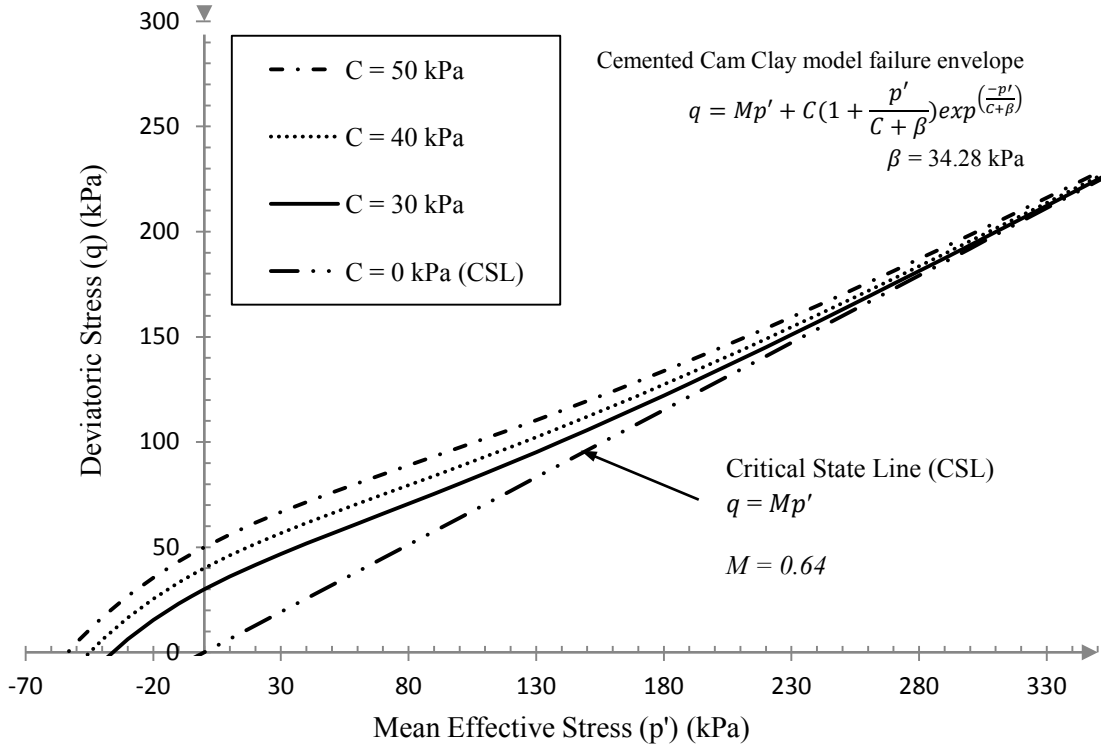

Figure 4. Effect of increasing cementation parameter (C) on the failure envelope of the proposed model

In contrast to the effect of increasing C on the failure envelope of CCC model, the degradation rate of cementation is reduced as β increases as shown in Figure 5. The effect of increasing β is insignificant on the shear strength of cemented clays in low mean effective stress range. However, the effect of β is more notable in high mean effective stresses. It should be noted that, when β decreases, the proposed failure envelope approaches the Critical State Line at a higher mean effective stress.

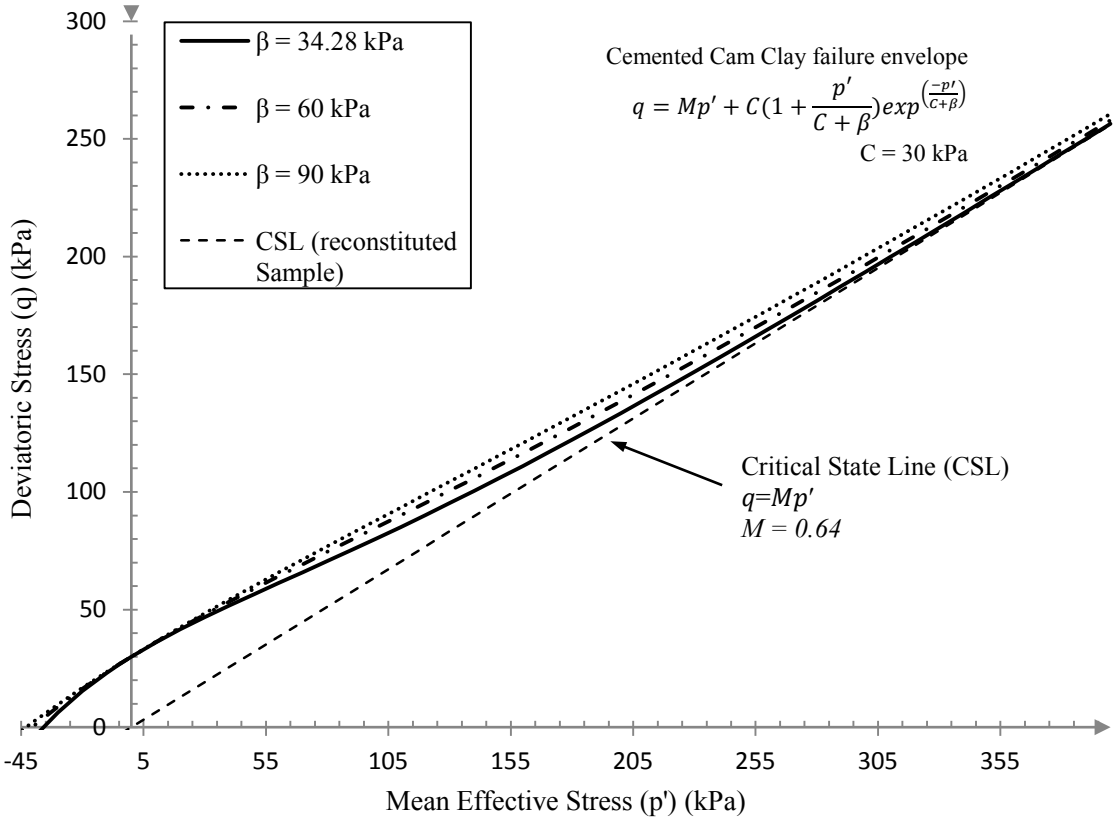

Figure 5. Effect of increasing $\boldsymbol{\beta}$ on the failure envelope of proposed model

3.3. Yield function

In the proposed model, cemented clay is assumed to be an isotropic material possessing elastic and virgin yielding behaviour. Following Modified Cam Clay (MCC) model, the yield function in $p' - q$ plane is described as:

$$f = q^2 - M^2 p'^* \left(p'^*_0 - p'^* \right) = 0 \tag{10}$$

where, $p'^*_0 = p'_0 + p'_\Omega$, p'^*_0 is the size of the yield surface where it meets with the horizontal axis (q = 0) in $p' - q$ plane, and p'_0 is a hardening parameter which corresponds to the mean effective stress (p') on the yield surface when q = 0. It should be noted that the virgin yielding occurs when stress state of the cemented clays is on the yield surface and with positive incremental change ($dp'^*_0 > 0$). The size of the initial yield surface, $p'^*_{0,i}$, is assumed to be equal to the initial mean effective yield stress, $p'^*_{y,i}$. The yield function with cementation is adopted to satisfy the critical state condition in which $\eta^* = 0$ when $p'^*_0 = p'^*$. The yield curve of the proposed model is taking the shape shown in Figure 6. The proposed yield function is different than that of MCC model by introducing the new function describing the effect of cementation (p'_Ω) which is influenced by the parameter *C*. Figure 7 displays the change in the shape of the proposed yield surface with variation of *C*. Increasing the value of parameter *C* results in expansion of the yield surface since p'_Ω increases. As depicted in Figure 7, when C = 0, the yield surface possesses elliptical shape similar to MCC model. Figure 8 displays the expansion in the proposed yield surface with an increase in the hardening parameter (p'_0). In addition, Figure 9 shows a shrinkage of the yield surface as the cementation degradation increases (reduction in β simulates degradation increase).

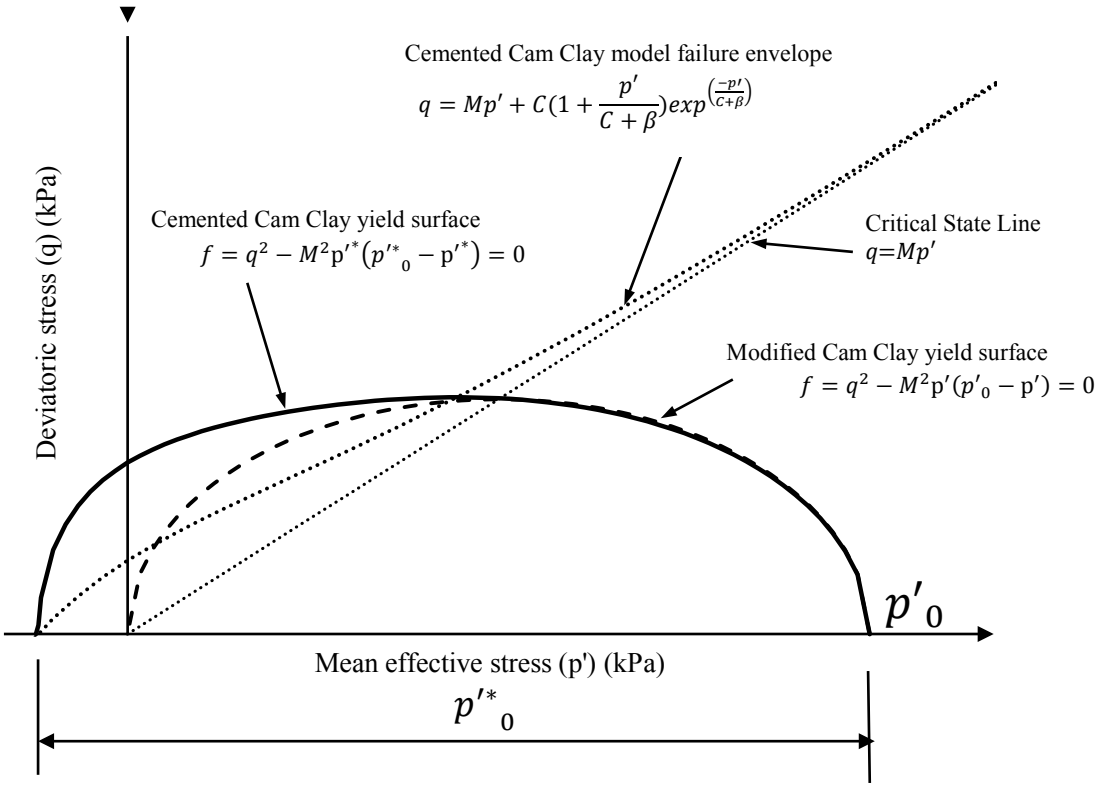

Figure 6. Cemented Cam Clay yield surface presented in this study

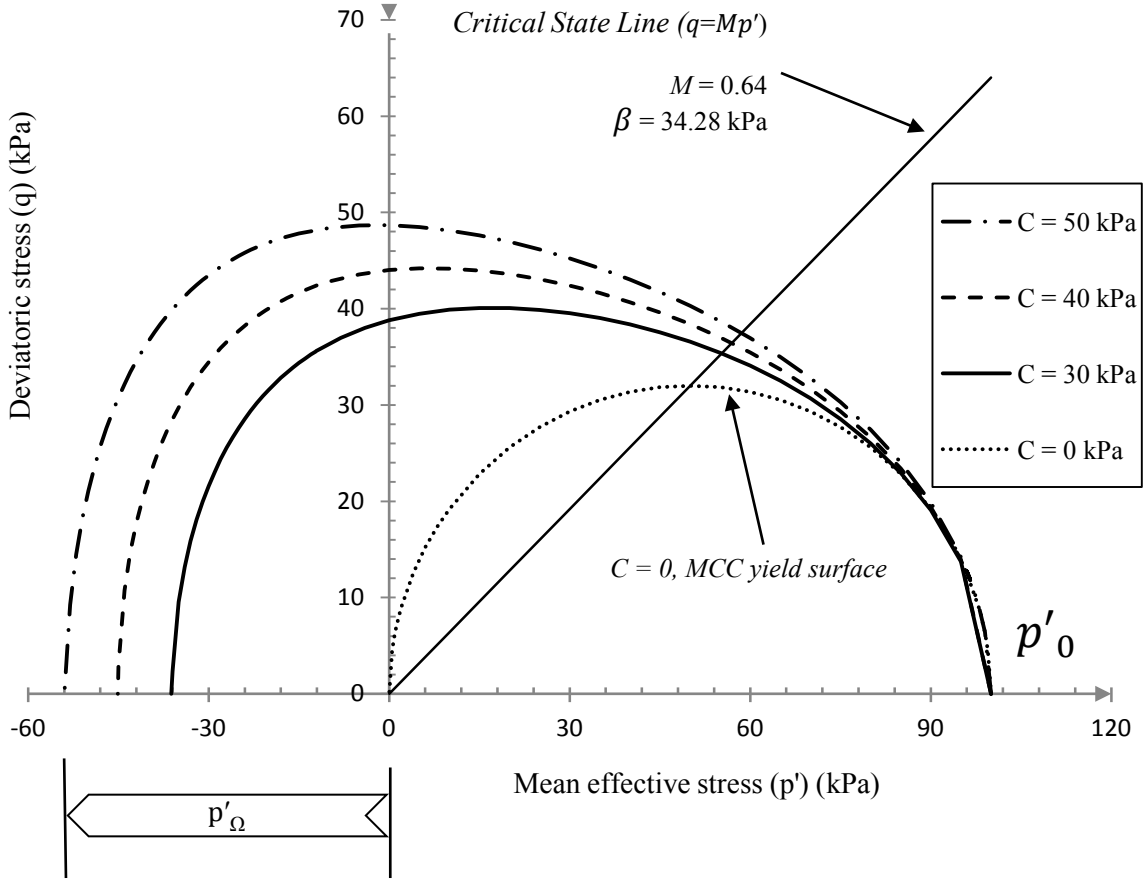

Figure 7. Proposed yield surface with increasing effect of cementation

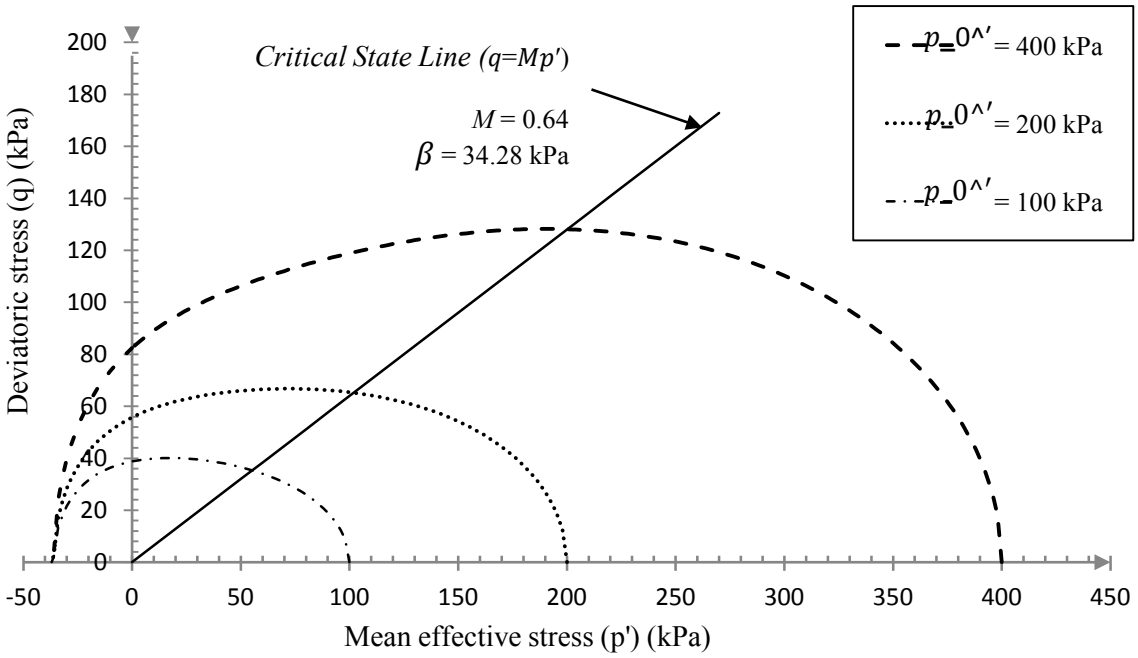

Figure 8. Proposed yield surface with increasing hardening parameter ($\boldsymbol{p_0'}$)

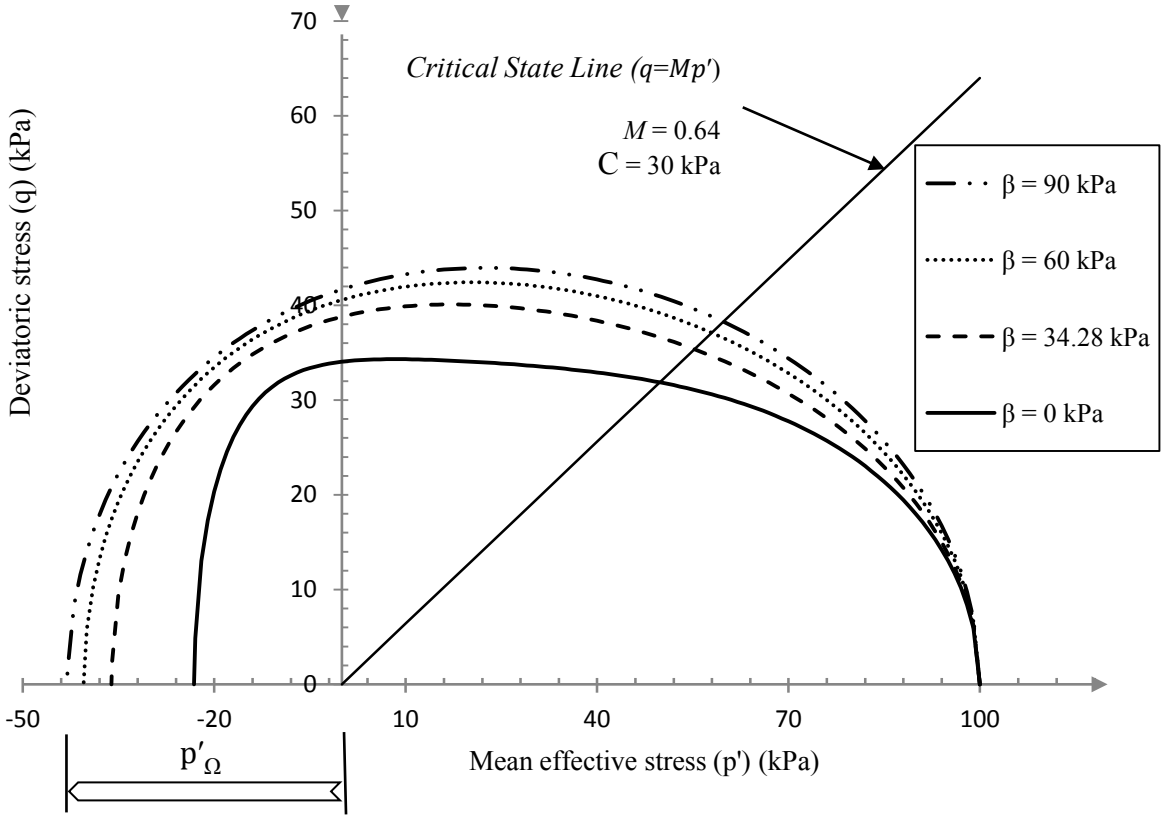

Figure 9.Proposed yield surface with variation of cementation degradation parameter (β)

3.4. The Energy Dissipation Equation

The internal plastic energy per unit volume (dW_{in}) available for dissipation of a soil sample in the triaxial test under the applied mean effective stress (p') and the shear stress (q) is expressed as (Wood and Graham, 1990):

$$dW_{in} = p' {d_v}^p + q {d_\varepsilon}^p \tag{11}$$

where, ${d_v}^p$ is the plastic volumetric strain increment and ${d_\varepsilon}^p$ is the plastic deviatoric strain increments.

MCC model assumes an expression for the dissipation of internal energy as follows (Roscoe and Burland, 1968):

$$p' {d_v}^p + q {d_\varepsilon}^p = p' \sqrt{({d_v}^p)^2 + (M {d_\varepsilon}^p)^2} \tag{12}$$

A more generalised equation of energy dissipation proposed by Kasama et al. (2000) is described by:

$$p' {d_v}^p + q {d_\varepsilon}^p = p' \sqrt{({d_v}^p)^2 + (M {d_\varepsilon}^p)^2 - X {d_v}^p {d_\varepsilon}^p} \tag{13}$$

The term $X {d_v}^p {d_\varepsilon}^p$ is described as the soil dilatancy dependent coupling term (Kasama et al., 2000). In this study, the authors attempt to make an appropriate selection for parameter X, leading to an appropriate energy dissipation equation for cemented clays capturing the effects of cementation and its degradation. The energy equation for cemented clay proposed in this study is presented in line with Equation (13) as:

$$p'^* {d_v}^p + q {d_\varepsilon}^p = p'^* \sqrt{({d_v}^p)^2 + (M {d_\varepsilon}^p)^2 + 2 \frac{q}{p'^*} {d_v}^p {d_\varepsilon}^p \left(1 - \frac{\alpha+1}{A}\right)} \tag{14}$$

$$A = \frac{d(p'^*)}{d(p')} = 1 - \frac{p' C}{M(\beta+C)^2} exp^{\left(\frac{-p'}{C+\beta}\right)} \tag{15}$$

$$X = -2 \frac{q}{p'^*} \left(1 - \frac{\alpha+1}{A}\right) \tag{16}$$

The expression for the term X is defined by the authors in Equation (16). The term A is introduced as the derivative of p'^* with respect to p'. There is a critical point on the failure curve of cemented clay afterwhich the failure curve approaches the failure line of

reconstituted clay-cement mixture (CSL) and by setting A = 0, this critical point can be defined. It should be noted that α is a non dimensional anisotropic parameter accounting for the coupling of deviatoric and volumetric plastic strain parameters.

For an isotropic compression case, where $q = 0$ and $d_\varepsilon{}^p = 0$, Equation (14) will reduce to:

$$dW_{in} = p'^* d_v{}^p \tag{17}$$

Moreover, on the Critical State Line, where $q = Mp'^*$ and $d_v{}^p = 0$, Equation (14) can be simplified as:

$$dW_{in} = p'^* M d_\varepsilon{}^p \tag{18}$$

It can be noted that when C = 0, and $\alpha = 0$, Equation (14) reduces to Equation (12) of MCC model. Moreover, due to the complexity of the proposed model and based on the semi-empirical method, the choice of X also depends on the simplicity of derivation of flow rules and the plastic potential function. It is also important to choose the energy dissipation equation and the X value in a way that Equations (17) and (18) are satisfied.

3.5. Flow Rule and Plastic Potential Function

The MCC model assumes an associated flow rule which is in the form $\left(\frac{d_v{}^p}{d_\varepsilon{}^p} = \frac{M^2-\eta^2}{2\eta}\right)$ so that the yield surface is also the plastic potential function. However, Bousshine et al. (2001) suggested that, in general, soil materials exhibit non-associated plastic flow rule as the strain parameter vectors are not normal to the yield locus. Due to the modified energy equation, the proposed model in this study assumes a non-associated flow rule which takes into account the effect of cementation and the curvature change of the failure envelope. By solving and rearranging the energy equation proposed in Equation (14) (see Appendix A), the flow rule of Cemented Cam Clay model is derived as follows:

$$\frac{d_v{}^p}{d_\varepsilon{}^p} = \frac{A\left[M^2-\eta^{*2}\right]}{2\eta^*(\alpha+1)} \tag{19}$$

The partial derivative of the modified stress ratio (η^*) (with respect to p' and q) can be presented in the following form:

$$d\eta^* = \frac{-q\left\{1-\frac{p'C}{M(\beta+C)^2}exp\left(\frac{-p'}{C+\beta}\right)\right\}}{\left[p'+\frac{C}{M}(1+\frac{p'}{C+\beta})exp\left(\frac{-p'}{C+\beta}\right)\right]^2}dp' + \frac{1}{p'+\frac{C}{M}(1+\frac{p'}{C+\beta})exp\left(\frac{-p'}{C+\beta}\right)}dq \quad (20)$$

Combining the proposed flow rule in Equation (19) with Equation (20) and taking integration to incorporate the boundary condition ($p' = p'_0$ when $q = 0$) , the plastic potential function (g) is derived as:

$$g = q^2(1+2\alpha) + M^2 p'^{*2}\left[1-\left(\frac{p'^*_0}{p'^*}\right)^{\left(\frac{2\alpha+1}{\alpha+1}\right)}\right] \quad (21)$$

A detailed derivation of the plastic potential function is included in Appendix A. In order to evaluate the effect of α, Figure 10 displays the shape of the plastic potential function (g) together with variations of α. When $\alpha = 0$, the plastic potential function coincides with the yield surface and consequently an associated flow rule is obtained.

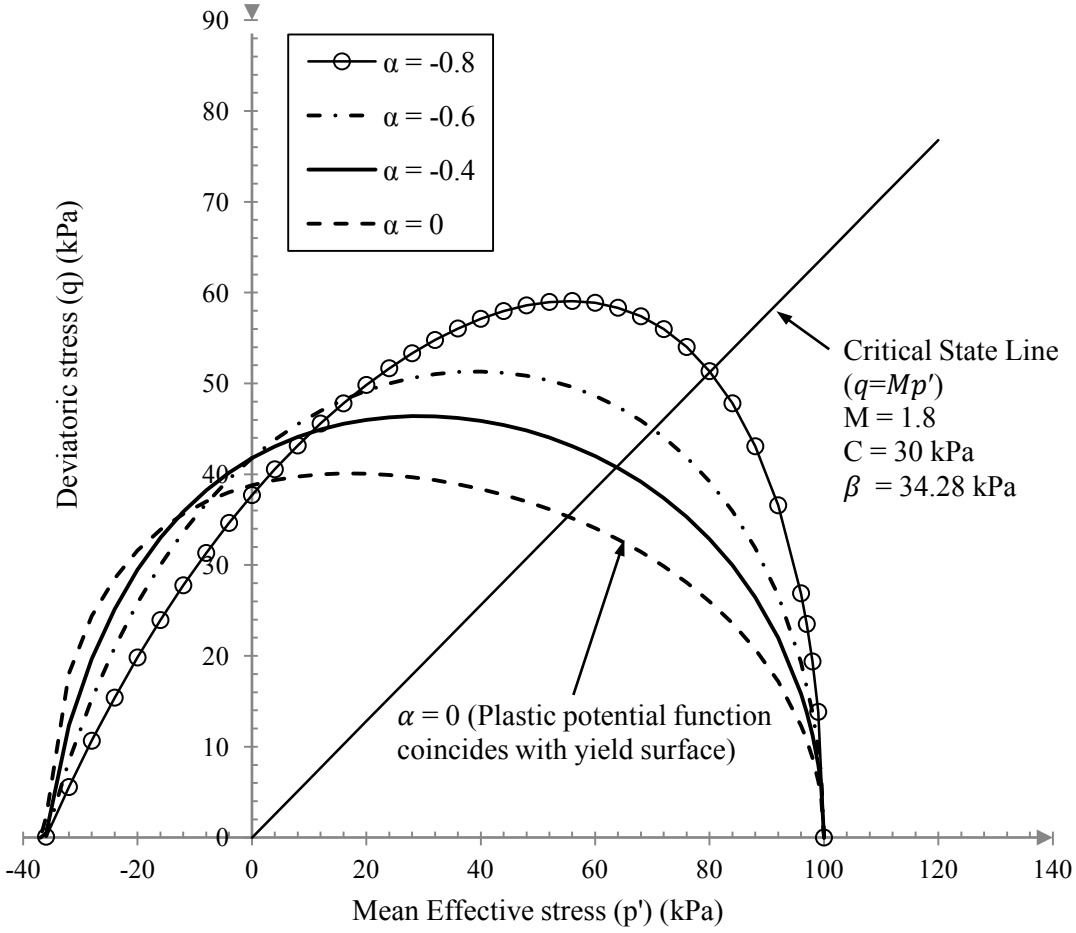

Figure 10.Plastic potential surface and the effect of increasing α

3.6. Elastic Deformation

When the stress state is within the yield surface, only elastic deformation occurs. Following the conventional MCC model, elastic deformation for soils is formulated following Hooke's Law widely adopted by many researchers such as Horpibulsuk et al. (2010); Perić and Ayari (2002) and Wood and Graham (1990). With the modified mean effective stress (p'^*), the proposed model also assumes an elastic deformation which is also dependent on the effect of cementation:

$$d_v{}^e = \frac{\kappa}{1+e}\left[\frac{d(p'^*)}{p'^*}\right] \tag{22}$$

$$d_\varepsilon{}^e = \frac{2\kappa(1+\nu)}{9(1-2\nu)(1+e)}\left[\frac{dq}{p'^*}\right] \tag{23}$$

where, $d_v{}^e$ is elastic volumetric strain increment, $d_\varepsilon{}^e$ is elastic deviatoric strain increment, ν is Poisson's ratio, κ is the elastic swelling/recompression index and e is the void ratio of the cemented clay. The adoption of this elastic deformation equation with relation to the modified mean effective stress is due to the experimental observations that the elastic deformation increases with the bond strength of cementation (Horpibulsuk et al., 2010).

3.7. Virgin Yielding Behaviour

Following the tradition of MCC model, the volumetric hardening law of the proposed model is expressed as:

$$\frac{dp'^*_0}{p'^*_0} = \frac{dp'^*}{p'^*} + \frac{d\eta^*}{(\eta^*+\psi^*)} \tag{24}$$

where, $\psi^* = \frac{d_v{}^p}{d_\varepsilon{}^p} = \frac{A\left[M^2-\eta^{*2}\right]}{2\eta^*(\alpha+1)}$, which is the slope of the current yield locus in $p'-q$ plane which is also called the flow rule as presented in Equation (19).

When the stress state of the cemented clays is on the yield surface and with $dp'^*_0 > 0$, virgin yielding occurs resulting to plastic deformations and it can be calculated adopting virgin isotropic consolidation line similar to MCC model. To predict the plastic deformation

of the cemented clay, the following equations are proposed for plastic volumetric strain increment ($d_v{}^p$) and plastic deviatoric strain increment ($d_\varepsilon{}^p$), respectively.

$$d_v{}^p = \frac{(\lambda-\kappa)}{1+e}\left[\frac{d(p'^*)}{p'^*} + \frac{2\eta^*(\alpha+1)d\eta^*}{2\eta^{*2}\alpha+M^2+\eta^{*2}}\right] \tag{25}$$

$$d_\varepsilon{}^p = \frac{(\lambda-\kappa)}{1+e}\left[\frac{d(p'^*)}{p'^*} + \frac{2\eta^*(\alpha+1)d\eta^*}{2\eta^{*2}\alpha+M^2+\eta^{*2}}\right]\frac{2\eta^*(\alpha+1)}{A\left(M^2-\eta^{*2}\right)} \tag{26}$$

where, λ is the slope of the normal compression line in $e - lnp'^*$ space. When the level of cohesion is diminished C = 0 and α is set to be 0, the proposed plastic deformation is reduced to MCC model which is in the form of:

$$d_v{}^p = \frac{(\lambda-\kappa)}{1+e}\left(\frac{d_p}{p} + \frac{2\eta d_\eta}{(M^2+\eta^2)}\right) \tag{27}$$

$$d_\varepsilon{}^p = \frac{(\lambda-\kappa)}{1+e}\left(\frac{d_p}{p} + \frac{2\eta d_\eta}{(M^2+\eta^2)}\right)\left(\frac{2\eta}{M^2-\eta^2}\right) \tag{28}$$

3.8. General Stress Strain Relationship

Combining Equations (22) and (25) yield the following equation to find the total volumetric strain increment (d_v):

$$d_v = d_v{}^e + d_v{}^p = \frac{1}{1+e}\left[\lambda\left(\frac{d(p'^*)}{p'^*}\right) + (\lambda-\kappa)\left(\frac{2\eta^*(\alpha+1)d\eta^*}{2\eta^{*2}\alpha+M^2+\eta^{*2}}\right)\right] \tag{29}$$

Furthermore, combining Equations (23) and (26) gives an equation to determine the total plastic deviatoric strain increment (d_ε), as:

$$d_\varepsilon = d_\varepsilon{}^e + d_\varepsilon{}^p = \frac{2\kappa(1+\nu)}{9(1-2\nu)(1+e)}\left[\frac{dq}{p'^*}\right] + \frac{(\lambda-\kappa)}{1+e}\left[\frac{d(p'^*)}{p'^*} + \frac{2\eta^*(\alpha+1)d\eta^*}{2\eta^{*2}\alpha+M^2+\eta^{*2}}\right]\frac{2\eta^*(\alpha+1)}{A\left(M^2-\eta^{*2}\right)} \tag{30}$$

When the stress state is increased to sufficiently high pressure, the contribution of cementation is diminished and $p'^* = p'$ (i.e. $p'_\Omega = 0$), and the derivative of p'^* presented by Equation (15) becomes 1. Thus, the proposed stress-strain relationship is reduced to that of MCC model.

4. ESTIMATION OF MODEL PARAMETERS

The proposed model involves nine major parameters. The following steps can be taken to predict the model parameters:

- The first five parameters including *M,* λ, κ, ν, and e are deemed to be reasonably independent of the soil structure induced by cementation and consequently can be determined same as the model parameter prediction procedure for MCC model, using a set of conventional isotropic compression tests. It should be noted that all these model parameters should be estimated for reconstituted clay-cement mixture. However, as reported by Horpibulsuk et al. (2010) and Liu and Carter (2002), these parameters can be reasonably estimated by reconstituted soil properties (excluding cement), particularly when small amount of chemical additives are used.
- Parameters C and β can be estimated using curve fitting to data obtained by plotting the peak shear stress of cemented clays in $p' - q$ space. In other words, Equation (9) should be fitted to the peak shear stress data (e.g. Figure 1) to obtain C and β. Parameter C indicates the shear strength when $p' = 0$, and β is the fitting parameter capturing the cementation degradation with the mean effective stress. Although data fitting is the most accurate method to determine these parameters, C can be estimated by the following equation as suggested by Horpibulsuk et al. (2010) and Liu and Carter (2002):

$$C = \frac{1}{2} q_u \tag{30}$$

where, q_u is the unconfined compressive strength of the cemented clays.

- The mean effective stress when virgin yielding occurs $\left(p'_{y,i}\right)$ is measured by linking it to the unconfined compressive strength (q_u) (Horpibulsuk et al., 2010; Liu and Carter, 2002). It can be estimated by $p'_{y,i} = q_u$.
- Parameter α, which is a non dimensional anisotropic variable, accounting for the coupling of deviatoric and volumetric plastic strain parameters, depends on the selection of the flow rule influencing the plastic potential function (g). The most appropriate α value results in the best fitted stress-strain curves, particularly in the post yielding stages. As explained earlier, assuming $\alpha = 0$ results in associated flow rule, meaning that the yield and the plastic potential surfaces overlap each other.

5. PERFORMANCE OF CEMENTED CAM CLAY MODEL

In this section, the performance of the Cemented Cam Clay model is evaluated by comparing the model prediction with available experimental data in literature. The three groups of test data including consolidated-undrained triaxial test results on cemented Aberdeen soil (reported by Sariosseiri (2008)), Singapore marine clay (reported by Kamruzzaman et al. (2009)) and Ariake clay (reported by Horpibulsuk et al. (2004)) are adopted in this study for verification exercise. The amount of cement content is calculated in percentage by a ratio of dry weight of cement and dry weight of clays (Horpibulsuk et al., 2004; Kamruzzaman et al., 2009; Sariosseiri, 2008). The model parameters have been obtained based on the procedure explained in Section 4. The adopted model parameters for the three selected cemented clays are summarised in Table 1.

Table 1. Values of model parameters for cemented clays

	Aberdeen soil treated with 5% Portland cement [a]	Singapore clay treated with 10% Portland cement [b]	Ariake clay treated with 6% Portland cement [c]
λ	0.162	0.73	0.446
κ	0.048	0.067	0.044
q_u (kPa)	534.3	300	78
e	1.97	2.85	4.37
υ	0.25	0.25	0.25
M	1.4	0.9	1.85
C (kPa)	267.15	150	39
β (kPa)	84	298	49
α	-0.6	-0.89	0.15

Laboratory data obtained from (a) Sariosseiri (2008), (b) Kamruzzaman et al. (2009), and (c) Horpibulsuk et al. (2004)

Figures 11-16 display a comparison among the CCC model predictions (the proposed model in this study), SCC model predictions (proposed by Horpibulsuk et al. (2010)) and available experimental data. It is observed that the CCC model predictions are in a good agreement with the experimental results, particularly in higher confining pressure ranges. Detailed discussions are presented below.

- Predicted and measured stress paths up to the peak shear strength for treated Aberdeen soil at 400 kPa and 600 kPa confining pressures are displayed in Figure 11. The stress path is initially within the yield surface and deformations are only elastic. However, when stress path reaches the yield surface (q = 336.25 kPa), the plastic deformation occurs. At the confining pressure of 600 kPa, it can be seen that the peak strength lies almost on the critical state line of the reconstituted soil as the cementation bonds were destroyed. It should be noted that SCC model is unable to capture this behaviour. Although, there are some disparities between the predicted stress – strain relationship at the initial stages of loading and laboratory measurements, the predictions begin to match up with the experimental data when the axial strain exceeds 1% as shown in Figure 12.

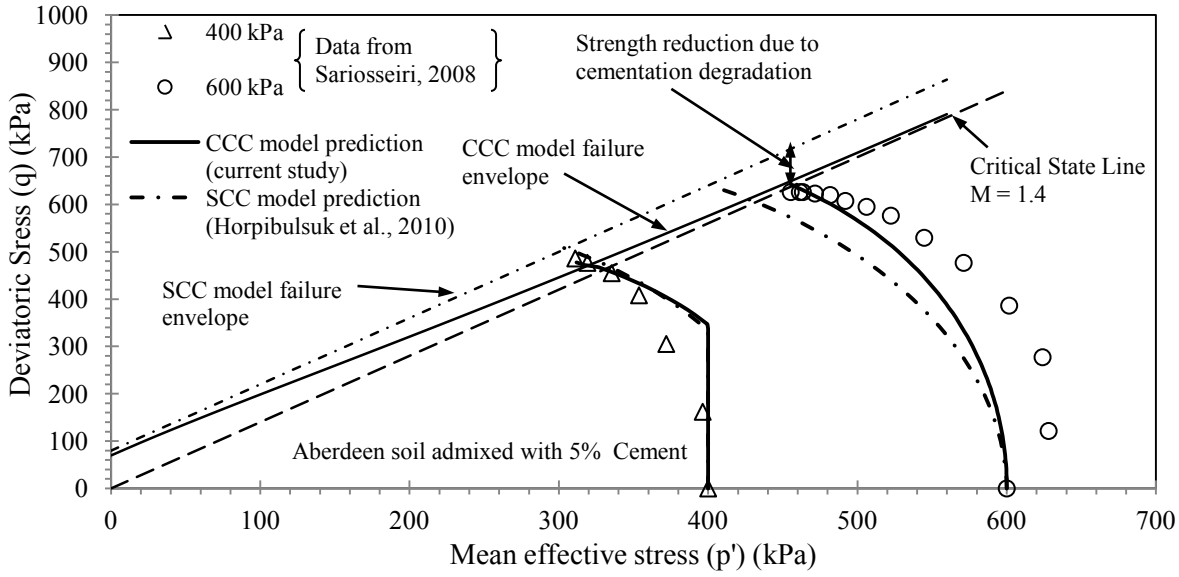

Figure 11.Undrained stress paths for Aberdeen Soil treated with 5% cement

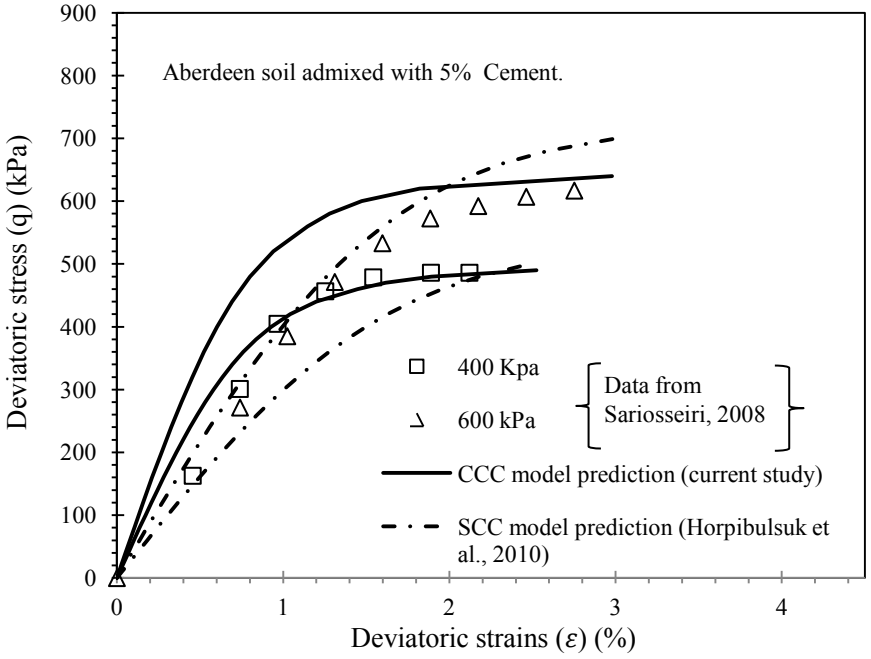

Figure 12. Stress and strain relationship of cemented Aberdeen soil with 5% cement content

- Kamruzzaman et al. (2009) performed a series of effective undrained triaxial tests on highly plastic Singapore marine clay admixed with 10% cement at different confining pressures ranging from 300 kPa to 1000 kPa. The undrained stress paths and the stress-strain relationship of Singapore clay are simulated in Figures 13 and 14, respectively. The proposed CCC model predictions for the cemented Singapore clay (at confining pressures of 500 kPa and 1000 kPa) are in very good agreement with measurements as noticed in Figures 13 and 14. The stress path at 1000 kPa is observed to be higher than the critical state line indicating that part of cementation is still present in the soil structure at the shearing stage.

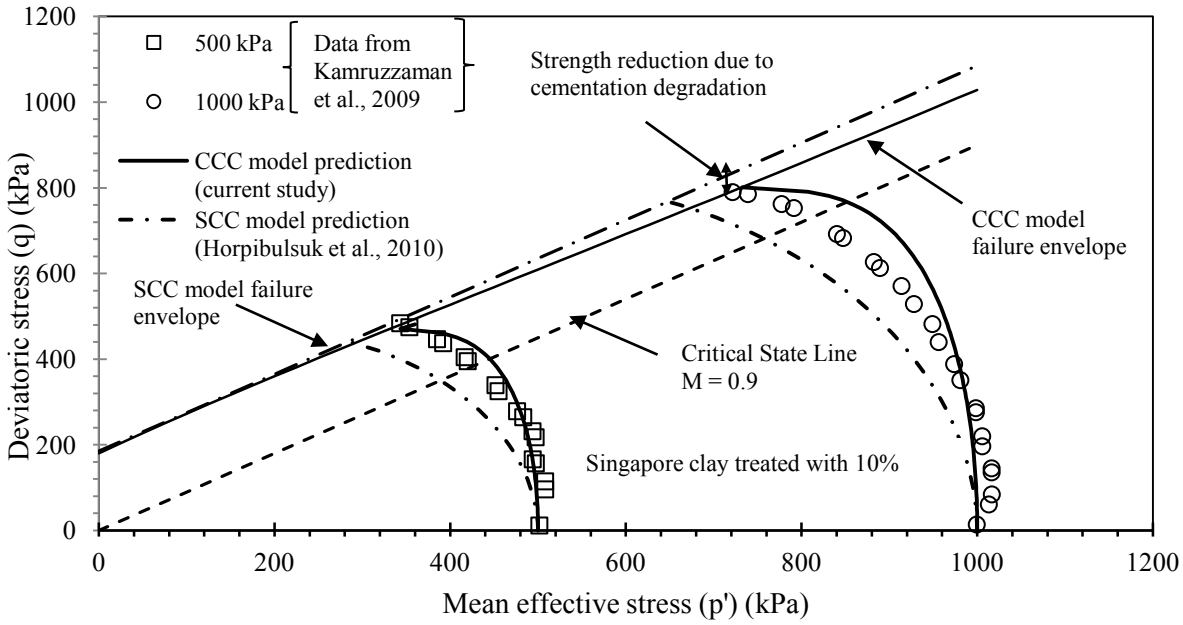

Figure 13.Undrained stress path for Singapore clay treated with 10% cement

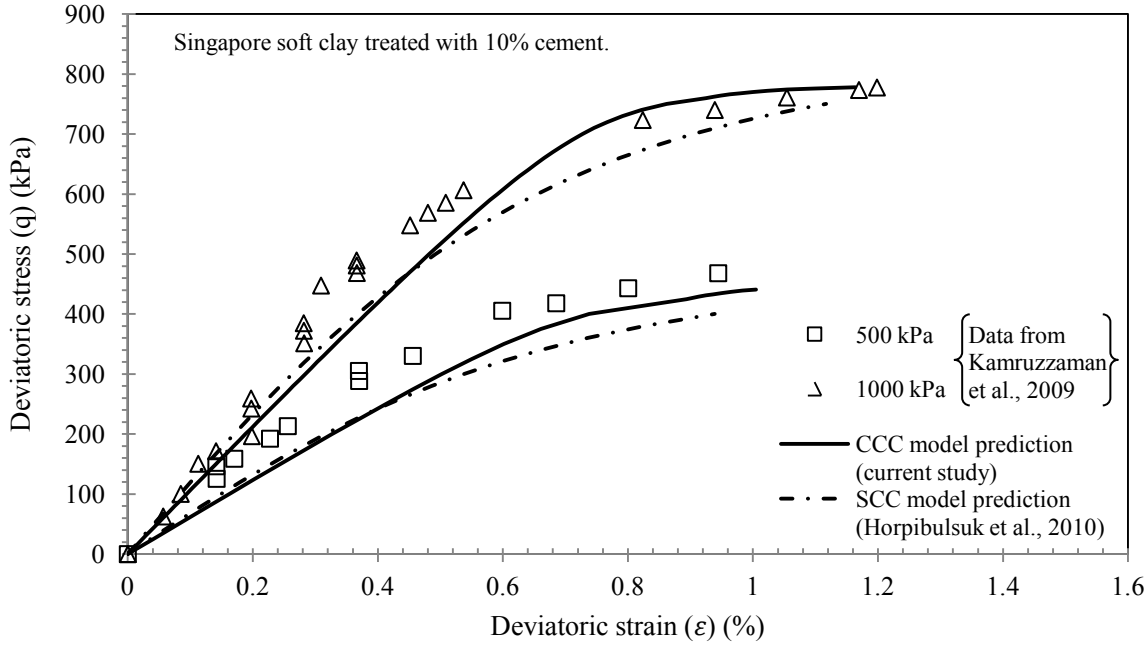

Figure 14.Stress strain relationship of Singapore clay treated with 10% cement

- Figures 15 and 16 display the comparison of CCC and SCC models for the consolidated-undrained triaxial tests data performed on Ariake clay admixed with 6% cement content reported by Horpibulsuk et al. (2004). The initial confining pressures of 100, 200, and 400kPa were adopted for testing. The virgin yielding occurs at 78kPa (q_u = 78 kPa), so the stress state of all samples is outside the yield surface. As observed in Figures 15 and 16, the results from CCC model provide a better prediction on the behaviour of treated Ariake clay than the predictions by SCC model particularly in higher confining pressure ranges.

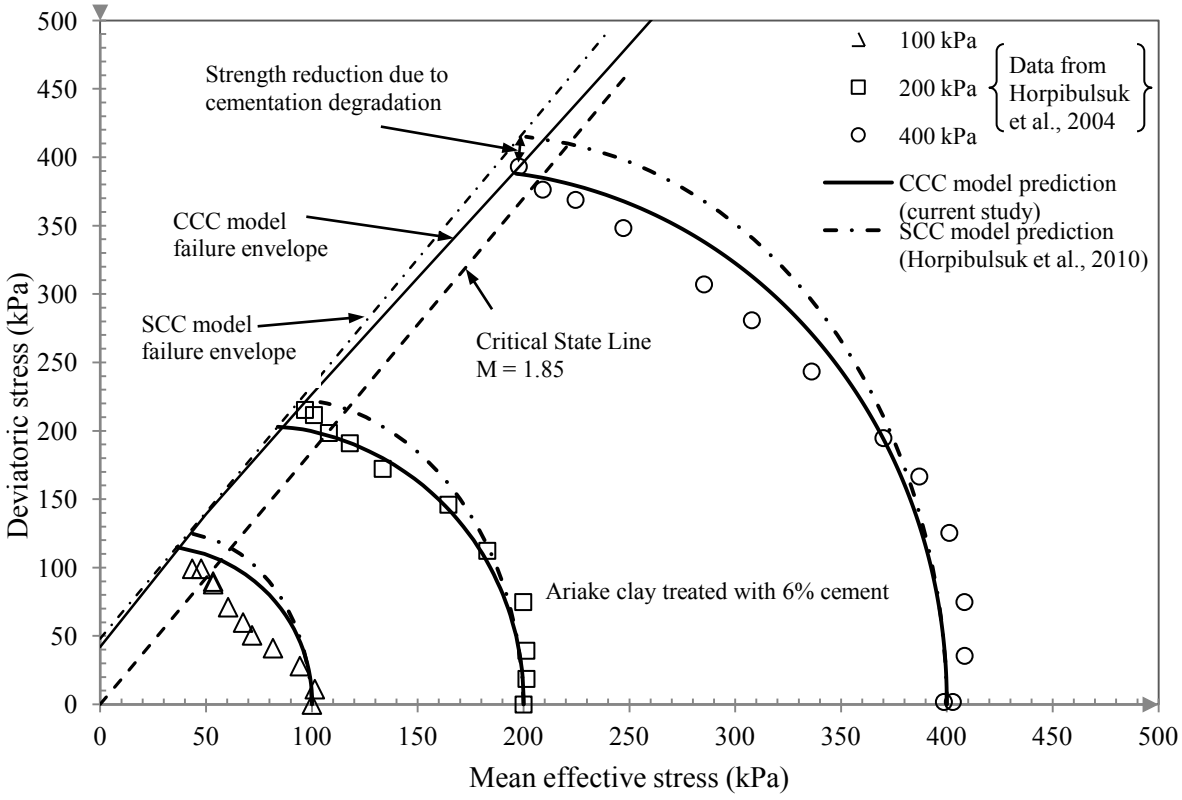

Figure 15.Undrained stress path of Ariake clay treated with 6% cement

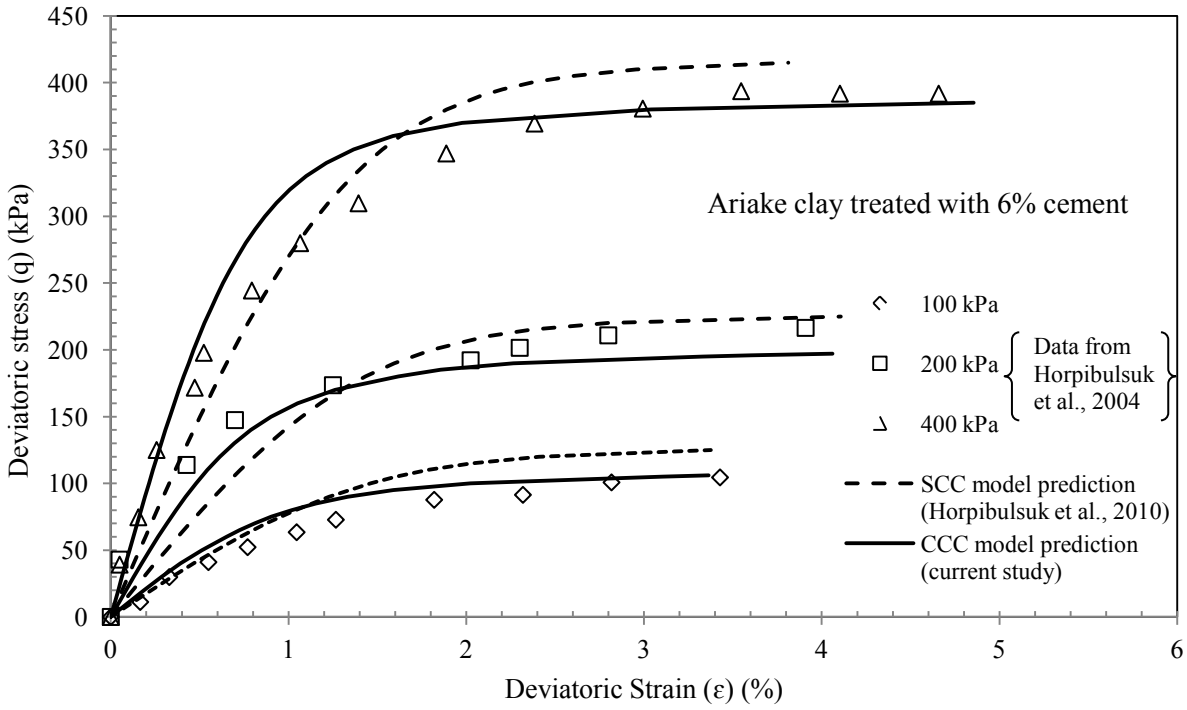

Figure 16.Stress and strain relationship of Ariake clay treated with 6% cement

6. DISCUSSION

When the effective confining pressure is on or outside the initial yield surface, the undrained effective stress path of cemented clays in $\boldsymbol{p' - q}$ plane initially rises upwards and bends towards to left and approaches the Critical State Line (CSL) of reconstituted cement-clay mixture indicating that plastic deformations occur as shown in the undrained stress paths of Aberdeen Soil (Figure 11), Singapore clay (Figure 13) and Ariake clay (Figure 15). This behaviour of cemented clay is similar to the normally consolidated soils, as observed by Horpibulsuk et al. (2010); Kasama et al. (2000); Uddin et al. (1997). The undrained stress paths continue to pass the CSL and reach a peak strength state as the effect of cementation is still present. However, the beneficial contribution of cementation to the peak shear strength $(\boldsymbol{q_u})$ of cemented clay is reduced as the effective confining pressure increases, due to the breaking of cementation bonds during shearing as illustrated in Figures 11, 13 and 15. For high effective confining stress ($\boldsymbol{p'_0}$ =600 kPa) in case of Aberdeen soil as shown in Figure 11 with low cement content (5%), the stress path reaches a peak strength state which lies on the CSL as the effect of cementation is completely destroyed. In addition, the failure envelope of cemented clay is clearly non-linear and gradually approaches the CSL of reconstituted cement-clay mixture as the effective confining pressure increases. The Structured Cam Clay (SCC) model ignores the reduction in the cementation contribution due to cementation degradation by adopting a linear failure envelope while the Cemented Cam Clay (CCC) model proposed in this paper captures this behaviour of cemented clays, thus provides a better agreement with experimental data.

7. CONCLUSION

The effective confining pressure plays a dominant role in the behaviour of cemented clays. Numerous laboratory experiments have indicated that the effect of cementation is diminished as the effective confining pressure is increased, due to degradation of cement-soil particle bonding. Various constitutive models were developed to simulate the behaviour of cemented clays, however the diminishing effect of cementation, particularly at high effective confining pressures is not captured in these models.

In this paper, a predictive constitutive model has been presented to simulate the behaviour of cemented clays referred to as Cemented Cam Clay model (CCC). The model failure envelope has been proposed in a way to merge with the Critical State Line of reconstituted clay-cement mixture, showing the diminishing effect of cementation due to degradation of cementation bonds when the confining pressure increases. The special characteristic of the proposed model includes a modified mean effective stress capturing cementation degradation. The main concepts and the formulations of CCC model, including a non-associated plastic potential function and elasto-plastic stress-strain relationship, have been presented within the framework of the critical state concept and inspired by Modified Cam Clay (MCC) model. It can be noted that when the effect of cementation is zero, the Cemented Cam Clay model is reduced to MCC model.

The performance of the proposed model has been evaluated by comparing experimental data available in literature with model predictions. Moreover, the predictions from Structured Cam Clay (SCC) model were also included as a comparison tool. The experimental data obtained from undrained triaxial tests performed on Aberdeen clay (admixed with 5% cement), Singapore clay (with 10% cement) and Ariake clay (with 6% cement) have been used in the validation of the proposed model. The results displayed a satisfactory performance of the proposed model and provided a good agreement with experimental data. The main features of the behaviour of cemented clay in undrained stress paths and stress-strain relationship, including the reduction in the cementation contribution in the peak shear strength and cementation degradation have been well captured in this model.

APENDIX A - Derivation of plastic potential function

Expanding and simplifying Equation (14) results in:

$$(qd_\varepsilon{}^p)^2 = p'^{*2}(Md_\varepsilon{}^p)^2 - 2p'^{*}qd_v{}^p d_\varepsilon{}^p\left(\frac{\alpha+1}{A}\right) \quad (A\text{-}1)$$

Dividing both sides by $d_\varepsilon{}^p$:

$$A(q^2 - p'^{*2}M^2)d_\varepsilon{}^p = -2p'^{*}q(\alpha+1)d_v{}^p \quad (A\text{-}2)$$

Rearranging Equation (*A-3*) to obtain the flow rule:

$$\frac{d_v{}^p}{d_\varepsilon{}^p} = \frac{A(q^2 - p'^{*2}M^2)}{-2p'^{*}q(\alpha+1)} \quad (A\text{-}3)$$

Substitutes the modified stress ratio $\left(\eta^* = \frac{q}{p'^*}\right)$ into Equation (*A-3*), the flow rule is taking the form of:

$$\frac{d_v{}^p}{d_\varepsilon{}^p} = \frac{A\left[M^2 - \eta^{*2}\right]}{2\eta^*(\alpha+1)} \quad (A\text{-}4)$$

Using the normality condition as follows:

$$\frac{d_v{}^p}{d_\varepsilon{}^p} = -\frac{dq}{dp'} \quad (A\text{-}5)$$

Adopting Equation (*15*) to obtain A in terms of p′and then combining Equations (*A-4*) and (*A-5*) results in:

$$-\frac{dq}{dp'} = \frac{\left\{1 - \frac{p'C}{M(\beta+C)^2}exp\left(\frac{-p'}{C+\beta}\right)\right\}\left[M^2 - \frac{q^2}{\left(p' + \frac{C}{M}(1+\frac{p'}{C+\beta})exp\left(\frac{-p'}{C+\beta}\right)\right)^2}\right]}{\frac{2q(\alpha+1)}{\left(p' + \frac{C}{M}(1+\frac{p'}{C+\beta})exp\left(\frac{-p'}{C+\beta}\right)\right)}} \quad (A\text{-}6)$$

It can be noted that Equation (*A-6*) is expressed in terms of p′. Substituting Equations (6) and (7) in Equation (8) results in:

$$\eta^* = \frac{q}{\left[p' + \frac{C}{M}(1+\frac{p'}{C+\beta})exp\left(\frac{-p'}{C+\beta}\right)\right]} \quad (A\text{-}7)$$

The equation for the partial derivatives of Equation (A-7) with respect to q and p′ is expressed as follows:

$$d\eta^* = \frac{\partial \eta^*}{\partial p\prime} dp' + \frac{\partial \eta^*}{\partial q} dq \qquad (A\text{-}8)$$

Evaluating the derivative of Equation (A-7) with respect to p' results in:

$$\frac{\partial \eta^*}{\partial p\prime} = \frac{-q\left\{1-\frac{p\prime C}{M(\beta+C)^2}exp^{\left(\frac{-p'}{C+\beta}\right)}\right\}}{\left[p'+\frac{C}{M}(1+\frac{p'}{C+\beta})exp^{\left(\frac{-p'}{C+\beta}\right)}\right]^2} \qquad (A\text{-}9)$$

Evaluating the derivative of Equation (A-7) with respect to q results in:

$$\frac{\partial \eta^*}{\partial q} = \frac{1}{\left[p'+\frac{C}{M}(1+\frac{p'}{C+\beta})exp^{\left(\frac{-p'}{C+\beta}\right)}\right]} \qquad (A\text{-}10)$$

Substituting Equations (A-9) and (A-10) in Equation (A-8) leads to:

$$\frac{dq}{dp\prime} = \left[p' + \frac{C}{M}(1 + \frac{p'}{C+\beta})exp^{\left(\frac{-p'}{C+\beta}\right)}\right]\frac{d\eta^*}{dp\prime} + \eta^*\left\{1 - \frac{p\prime C}{M(\beta+C)^2}exp^{\left(\frac{-p'}{C+\beta}\right)}\right\} \qquad (A\text{-}11)$$

Substituting the flow rule presented in Equation (*A-6*) into Equation (*A-11*) and then integrating the equation using the boundary conditions ($p' = p'_0$ when $q = 0$) results in the plastic potential function as follows:

$$g = q^2(1 + 2\alpha) + M^2 p'^{*2}\left[1 - \left(\frac{p'^*_0}{p'^*}\right)^{\left(\frac{2\alpha+1}{\alpha+1}\right)}\right] \qquad (A\text{-}12)$$

REFERENCES

Bousshine, L., Chaaba, A., De Saxcé, G., 2001. Softening in stress–strain curve for Drucker–Prager non-associated plasticity. International Journal of Plasticity 17, 21-46.

Chew, S.H., Kamruzzaman, A.H., Lee, F.H., 2004. Physicochemical and engineering behavior of cement treated clays. Journal of geotechnical and geoenvironmental engineering 130, 696-706.

Diamond, S., Kinter, E.B., 1965. Mechanisms of soil-lime stabilization. Highway research record, 83-102.

Horpibulsuk, S., Liu, M.D., Liyanapathirana, D.S., Suebsuk, J., 2010. Behaviour of cemented clay simulated via the theoretical framework of the structured cam clay model. Computers and Geotechnics 37, 1-9.

Horpibulsuk, S., Miura, N., Bergado, D.T., 2004. Undrained shear behavior of cement admixed clay at high water content. Journal of geotechnical and geoenvironmental engineering 130, 1096-1105.

Kamruzzaman, A.H., Chew, S.H., Lee, F.H., 2006. Microstructure of cement-treated Singapore marine clay. Proceedings of the ICE-Ground Improvement 10, 113-123.

Kamruzzaman, A.H., Chew, S.H., Lee, F.H., 2009. Structuration and Destructuration Behavior of Cement-Treated Singapore Marine Clay. Journal of geotechnical and geoenvironmental engineering 135, 573-589.

Kasama, K., Ochiai, H., Yasufuku, N., 2000. On the stress-strain behaviour of lightly cemented clay based on an extended critical state concept. Soils and Foundations 40, 37-47.

Lade, P.V., Overton, D.D., 1989. Cementation effects in frictional materials. Journal of Geotechnical Engineering 115, 1373-1387.

Liu, M.D., Carter, J.P., 2002. A structured Cam Clay model. Canadian Geotechnical Journal 39, 1313-1332.

Lo, S., Wardani, S., 1999. Deformation Behaviour of Cement-flyash Stabilised Silt, Proceedings 8th Australia New Zealand Conference on Geomechanics: Consolidating Knowledge. Australian Geomechanics Society, p. 761.

Lorenzo, G.A., Bergado, D.T., 2006. Fundamental characteristics of cement-admixed clay in deep mixing. Journal of materials in civil engineering 18, 161-174.

Moses, G.G., Rao, S.N., Rao, P.N., 2003. Undrained strength behaviour of a cemented marine clay under monotonic and cyclic loading. Ocean engineering 30, 1765-1789.

Panda, A.P., Rao, S.N., 1998. Undrained strength characteristics of an artificially cemented marine clay. Marine georesources & geotechnology 16, 335-353.

Perić, D., Ayari, M.A., 2002. On the analytical solutions for the three-invariant Cam clay model. International Journal of Plasticity 18, 1061-1082.

Porbaha, A., 1998. State of the art in deep mixing technology. Part I: Basic concepts and overview. Ground Improvement 2, 81-92.

Porbaha, A., Shibuya, S., Kishida, T., 2000. State of the art in deep mixing technology. Part III: Geomaterial characterization. Proceedings of the ICE-Ground Improvement 4, 91-110.

Roscoe, K.H., Burland, J.B., 1968. On the generalised stress-strain behaviour of" wet" clay. Engineering Plasticity, 535-609.

Sariosseiri, F., 2008. Critical state framework for interpretation of geotechnical properties of cement treated soils. Washington State University, Pullman.

Sariosseiri, F., Muhunthan, B., 2009. Effect of cement treatment on geotechnical properties of some Washington State soils. Engineering Geology 104, 119-125.

Tan, T.S., Goh, T.L., Yong, K.Y., 2002. Properties of Singapore marine clays improved by cement mixing. ASTM geotechnical testing journal 25, 422-433.

Uddin, K., Balasubramaniam, A.S., Bergado, D.T., 1997. Engineering behavior of cement-treated Bangkok soft clay. Geotechnical Engineering 28, 89-119.

Wood, D., Graham, J., 1990. Anisotropic elasticity and yielding of a natural plastic clay. International Journal of Plasticity 6, 377-388.

Yasufuku, N., Ochiai, H., Kasama, K., 1997. The dissipated energy equation of lightly cemented clay in relation to the critical state model, Procceedings 9th International Conference on Computer Methods & Advances in Geomechanics, pp. 917-922.

Yin, J.-H., 2001. Stress-strain-strength characteristics of soft Hong Kong marine deposits without or with cement treatment. Lowland Technology International 3, 1-13.

List of Figures